Benajes Calvo, JV.; Molina Alcaide, SA.; García Martínez, A.; Monsalve Serrano, J.; Durrett, R. (2014). Performance and engine-out emissions evaluation of the double injection strategy applied to the gasoline partially premixed compression ignition spark assisted combustion concept. Applied Energy. 134:90-101. doi:10.1016/j.apenergy.2014.08.008.

PERFORMANCE AND ENGINE-OUT EMISSIONS EVALUATION OF THE DOUBLE INJECTION STRATEGY APPLIED TO THE GASOLINE PARTIALLY PREMIXED COMPRESSION IGNITION SPARK ASSISTED COMBUSTION CONCEPT

Jesús Benajes[a], Santiago Molina[a], Antonio García[a], Javier Monsalve-Serrano[a] and Russell Durrett[b]

a - CMT - Motores Térmicos, Universitat Politècnica de València, Camino de Vera s/n, 46022 Valencia, Spain

b - Diesel Engine Systems Group, Propulsion Systems Research Lab GM R&D Center, MC 480-106-252, 30500 Mound Rd., Warren, MI 48090-905, USA

(*) CORRESPONDING AUTHOR:

Dr. Antonio Garcia: angarma8@mot.upv.es

Telephone: +34 963879659

Fax: +34 963877659

ABSTRACT

Spark assistance has been found to improve combustion control when combined with both single and double injection operation applied to compression ignition (CI) engines using gasoline as the fuel. Previous work has verified the potential of a double injection strategy when applied to the gasoline spark assisted partially premixed compression ignition combustion (PPC) concept. The current research presents performance and engine-out emissions results using a double injection strategy with the spark assisted PPC concept and shows its benefits compared to a single injection strategy. For this purpose, a parametric study was carried out using gasoline in a high-speed single-cylinder diesel engine equipped with a modified cylinder head, which included a spark plug. The parameters that were varied during the double injection testing included: injection timing, dwell, fuel mass split between the injections and intake oxygen concentration. A detailed analysis of the air/fuel mixing process was also conducted by means of a 1-D in-house spray model (DICOM).

KEYWORDS

Partially premixed combustion

Spark assistance

High octane number gasoline

Double injection

Performance and engine-out emissions

1. INTRODUCTION

Along the last years, engine researchers are more and more focusing their efforts on the advanced low temperature combustion (LTC) concepts with the aim of achieving the stringent limits of the current emission legislations. In this regard, strategies based on highly premixed combustion such as the well-known Homogeneous Charge Compression Ignition (HCCI) have been confirmed as a promising way to decrease drastically the most relevant CI diesel engine-out emissions, NOx and soot [1]. However, the major HCCI drawbacks are the narrow load range, bounded by either misfiring (low load, low speed) or hardware limitations (higher load, higher speeds) and the combustion control (cycle-to-cylce control and combustion phasing). Although several techniques such as EGR [2], variable valve timing [3][4], variable compression ratio [5] and intake air temperature control [6] have been widely investigated in order to overcome these drawbacks, the high chemical reactivity of the diesel fuel remains as the main limitation for the combustion control.

The attempts of the researchers to overcome these disadvantages are shifting to the use of fuels with different reactivity [7]-[9]. Specifically, the use of gasoline-like fuels with high autoignition resistance in compression ignition engines has been widely investigated at Shell [10]-[13], Lund [14]-[17], UW-Madison [18]-[22] and Argonne [23]-[25]. In this sense, the concept of gasoline Partially Premixed Combustion has been able to reduce emissions and improve efficiency simultaneously, but some drawbacks still need solution. Since a low reactive fuel is required to extend the ignition delay sufficiently at high loads, controllability and stability issues appear at the low load end. Thus, with the aim of improving the PPC controllability and stability at low load, the PPC concept with spark assistance fuelled with gasoline has been studied [26][27]. This combustion concept has been evaluated in terms of performance and engine-out emissions using a single injection strategy by studying the effect of injection pressure variations and intake oxygen concentration. Under these conditions, the concept has been found as a suitable technique for improving combustion control, providing both temporal and

spatial control over the combustion process [28]. In spite of its benefits, some drawbacks related to unappropriated mixture distribution and combustion temperatures were observed. Single injection provides excessive rich zones near the spark plug and too lean regions close to the in-cylinder walls resulting in high emission levels as well as deteriorated Fuel energy Conversion Efficiency (FeCE).

Another strategy widely investigated by several researchers with the aim of solving the gasoline PPC controllability and stability issues encountered when using single injection strategies at low load is the use of multiple injection strategies, which improve the control over the fuel/air mixture preparation before SOC. Thus, some level of mixture stratification in the chamber has been shown necessary to improve low load operation. The double injection strategy provides sufficient mixing time before the SOC to achieve a homogeneous charge as well as the reactive conditions required to trigger the combustion process, improving the combustion stability. However, to achieve auto-ignition time scales small enough for combustion in the engine, an increase in the intake pressure and temperature is required [29]. In addition, recent studies with multiple injections have shown that fuels with octane number greater than 90 do not allow to run below 5 bar BMEP load [30] due to the auto-ignition characteristics of these fuels. In this regard, previous work from the authors [28] showed the capability of the spark plug to provide combustion control in engine loads below this limit even using 98 octane number gasoline. Thus, the main objective of the present work is to couple the control capability of the spark assistance together with an appropriate mixture distribution by using double injection strategies with the aim of evaluating performance and engine-out emissions at low load PPC range using a high octane number gasoline. For this purpose different parameters have been varied during the double injection testing, specifically: injection timing, dwell time between injections, fuel mass repartition between injections and intake oxygen concentration. The investigation has been performed in a compression ignition single-cylinder engine to allow high compression ratio fuelled with 98 octane number gasoline. A common rail injection system enabling high injection pressures has been used during

the research. An analysis of the in-cylinder pressure signal derived parameters as well as a detailed analysis of the air/fuel mixing process by means of a 1-D in-house spray model (DICOM) has been conducted [31].

The outline of this paper is as follows: in the next section, the experimental facilities used to carry out this research are presented. Specifically, this section describes briefly the methodology, hardware and processing tools. In section 3, an overview of the double injection strategy is given by presenting a comparison of the single and double injection strategies using different operating conditions. In section 4, the results of the double injection strategy tests are presented. These tests consist of sweeps of the pilot injection timing and the intake oxygen concentration. Then, the effects of the mass repartition between the pilot and main injection are studied. Finally, in section 5, the main conclusions of this research are summarized.

2. MATERIAL AND METHODS

This section describes the methodology used to acquire the experimental data and provides a description of the experimental facility, the different devices and systems that were specifically adapted for the study of this combustion mode.

2.1. Single cylinder engine

The engine used in the present study is a 4-valve, 0.545 l displacement single cylinder engine with a modified cylinder head for the study of this combustion mode. The bowl dimensions are 45x18 mm (diameter x depth). Table 1 presents the main characteristics of the engine.

A spark plug is required to implement the partially premixed compression ignition with spark assistance combustion mode. As Figure 1 shows, the cylinder head has been modified by removing an exhaust valve and thus enabling the insertion of the spark plug in the combustion chamber. A standard spark plug (*Veru Platinum*) with a 1 mm gap is used along with a custom electronic control system. In the

standard configuration, the tip protrudes 4.5 mm into the combustion chamber from the cylinder head plane and it is located 17 mm from the cylinder axis. The injector is centered and vertically assembled in the modified cylinder head with a graduated metal circle that can change the relative position between the spark plug and the injector fuel jets by rotating the injector around its vertical axis. This relative position is fixed to make the spray pass between the spark electrodes.

In order to increase the reliability of the combustion mode, a Delphi multicharge ignition system has been used. The high amount of energy released by this ignition system allows igniting the mixture even with local equivalence ratio conditions near their flammability limits with high EGR rates. The spark ignition system is operated at a constant nominal primary voltage of 15 V from the battery and primary current of 25 A, providing around 120 mJ for the typical combustion chamber density test conditions, almost double than a conventional ignition system.

In order to characterize the most relevant properties of the gasoline used in this research, various analyses of the fuel properties have been performed following ASTM standards. It is worthy to note that 300 ppm of additive (*Havoline Performance Plus*) was added to improve the lubricity of the gasoline up to diesel fuel level, increasing the service life of the high pressure pump and fuel injector. The addition of the additive does not modify neither density nor the viscosity. The results of the gasoline characterization are summarized in Table 1.

The fuel injection system is based on an electronically controlled Bosch common rail system. The injector is a *Bosch* piezoelectric *CRIP 3.3* model equipped with a seven-hole nozzle with 154° included angle. The nozzle hole diameter is 97 microns and its flow capacity is 210 cm^3/30 s. The injection control system makes it possible to modify any parameter of the injection events such as the start of injection timing, injection duration and rail pressure. The injector is centered in the cylinder and vertically mounted in the modified cylinder head with a graduated metal circle that can be used to change the

relative position between the spark plug and the injector by rotating the latter around its vertical axis. The fuel injection hardware characteristics are sumarized in Table 1.

2.2. Test cell

This section presents the experimental configuration of the test cell and the main subsystems used in this study. As Figure 2 shows, the single cylinder engine is installed in a fully instrumented test cell, with all the auxiliary facilities required for operation and control.

The intake air is supplied by a roots compressor with an upper pressure limit of 3 bar. Then, the air flows through a filter to remove possible impurities. The heat exchanger and the air dryer allow controlling the temperature and humidity of the intake air independently of the ambient conditions. The temperature in the inlet settling chamber is maintained constant by using a heater in the intake line. The oxygen concentration variation is performed using a synthetic EGR system. EGR is substituted by nitrogen gas, which greatly simplifies the system ensuring a controllable gas composition without an excessive time to adjust the facility. Despite the limited practical application, it was decided to use this method to have a better control of the variables, which allows studying the underlying phenomena more carefully. The concept is based on decreasing the O_2 concentration at the inlet manifold by increasing the flow of N_2 and keeping constant the total intake mass flow rate (substitution EGR). For this purpose a PID controller is equipped to operate the N_2 valve governed by the intake O_2 meter. With this system, the in-cylinder thermodynamic conditions can be reproduced systematically. To ensure a homogeneous mixture of N_2 and O_2 and to attenuate pressure pulses in the intake manifold, a settling chamber of 500 liters volume is used in the installation.

The exhaust gases were analysed by a Horiba MEXA 7100 D. In order to increase the robustness of these measurements, the different pollutant volume fractions were sampled and averaged over an 80 second time period. Smoke emissions were measured with an AVL 415 variable sampling smoke meter,

providing results directly in FSN. The FSN values used in this research are the average of three consecutive measurements at the same operating condition. These measurements were transformed into mg/m3 by means of the correlation proposed in the user manual of the device:

$$\left[\mathbf{mg/m^3}\right] = \frac{\mathbf{1}}{\mathbf{0.405}} \cdot \mathbf{4.95} \cdot \mathbf{FSN} \cdot \mathbf{e^{0.38 \cdot FSN}} \qquad (1)$$

In the exhaust line, after the exhaust analyzer sample probe, a catalyst is mounted to prevent the accumulation of unburned hydrocarbons in the installation. Due to the low temperatures achieved during the combustion event and therefore in the exhaust line, the catalyst is often operating with low efficiency and a cyclone is needed to remove the rest of the hydrocarbons. In the same way as in the intake line, a settling chamber is mounted in order to attenuate pressure pulses. Finally, an exhaust backpressure valve is equipped to maintain a relative pressure of 0.2 bar to the intake pressure, in order to simulate more realistic conditions.

The in-cylinder pressure traces from a piezo-electric transducer (*Kistler 6067C1*) were recorded during 200 engine cycles in order to compensate the cycle-to-cycle variation during the engine operation. The recorded values of in-cylinder pressure were processed by means of an in-house one-zone combustion diagnosis code (CALMEC) [32], which provides valuable information such as the rate of heat release (RoHR) and the unburned gases temperature. To obtain these results, the first law of thermodynamics is applied between IVC and EVO, considering the combustion chamber as an open system because of blow-by and fuel injection. The ideal gas equation of state is used to calculate the mean gas temperature in the chamber. Along with these two basic equations, several sub-models are used to calculate instantaneous volume and heat transfer [33], among other things. The main result of the model is the Rate of Heat Release (RoHR), which is obtained from a filtered and averaged in-cylinder pressure signal. Information related to each cycle can be obtained, such as the IMEP and SoC. Start of Combustion (SoC) is defined as the crank angle position in RoHR where the beginning of the slope rise

due to combustion is detected. Additionally, the knocking level is calculated by using the Integrate Modulus of Pressure Gradient (IMPG) method [34]-[37]. This method was selected considering that the combustion mode presented in the current paper is a transition between a spark ignition and compression ignition engine. The IMPG knocking level is proportional to the ringing intensity estimator which is more commonly used in CI combustion under fully or partially premixed combustion modes. The IMPG method applies a FFT and a band pass filter in the range of 5 to 20 kHz in order to determine fluctuations in the cylinder pressure signal over a certain crank angle degree range. Once the crank angle interval is defined, the knocking level is calculated as:

$$\mathrm{IMPG} = \frac{1}{\mathrm{N}} \sum_{1}^{\mathrm{N}} \int_{\alpha_0}^{\alpha_1} \left| \frac{\mathrm{dp}}{\mathrm{d}\alpha} \right| \mathrm{d}\alpha = \frac{1}{\mathrm{N}} \sum_{1}^{\mathrm{N}} \sum_{\alpha_0}^{\alpha_1} |\Delta \mathrm{p_i}| \qquad (2)$$

Values of IMPG over 50 imply an excessive knocking level.

2.3 1-D Spray model

A 1-D in-house spray model DICOM is used to estimate equivalence ratio distributions in the fuel jet in order to get better insight into the variations in mixture distribution associated with the variations in the parameters studied in the experimental tests. The start of combustion and the combustion development have an extreme dependency on the local mixture conditions at Start of Spark (SoS) timing. The inputs of the DICOM model are the in-cylinder thermodynamic conditions (pressure, temperature and density), the spray cone angle, the fuel mass flow rate and the spray momentum. The model solves the general conservation equations either in a transient or steady state formulation for axial momentum and fuel mass along the center line. The results can be used to calculate values of spray velocity, species mass fractions and other values of the mixing process [38]. Finally, with some other assumptions described in [31], the model is used to obtain different temporal evolutions such as the spray liquid and vapor penetration, maximum spray velocity, equivalence ratio along the center line of the spray and the fuel

mass fraction which has mixed to different equivalences ratios. The fuel mass fraction is the main variable used in this research.

3. PRELIMINARY RESULTS: EMISSIONS AND PERFORMANCE

In this section, preliminary results of tests using the single and double injection strategies will be presented. Table 2 shows the different operating conditions that were tested in order to have an overview of the double injection strategy's potential. In order to comprehend the PPC with spark assistance combustion development, previous work using the transparent engine version [26] has been carried out. The PPC with spark assistance combustion process sequence can be summarized as follows: Once the injection event has finished, the spark plug discharge takes place initiating the combustion process. The kernel growth generates a partially premixed flame propagation guided by the swirl motion which energy release causes an increase in the unburned gas pressure and temperature, leading finally to a second phase of combustion governed by the autoignition of the rest of the mixture. In addition, the effect of the injection pressure and the intake XO_2 variation on the combustion mode as well as the performance and engine-out emissions using single injection strategies has been studied in [28].

Figure 3 shows some of the previous results in terms of soot, CO, HC and ISFC versus NOx for SoI=-24 CAD aTDC using single injection and also for the double injection strategy tests depicted in Table 2. For each single injection strategy operating condition, the global equivalence ratio is increased from the left to the right with the extremes points corresponding to the maximum and minimum values depicted in Table 2.

It is noticeable that for all the points presented in Figure 3, regardless of the engine settings, the engine-out NOx levels are unacceptable taking into account the current regulations. In this combustion mode, one of the main sources of NOx formation is tied to the way in which the mixture ignition and the initial

premixed flame phase propagation is achieved. The initial kernel ignition must take place in a mixture that is near stoichiometric conditions in order to allow the flame to grow. As the premixed flame propagates through this region it promotes high temperature combustion products which are significantly above the mean temperature. The high temperature in these products of the initial flame propagation causes significant NOx production.

The double injection strategy seems to be a good strategy to reduce the NOx levels. Since the pilot is injected earlier in the cycle (SoI_{pilot}= -16 CAD aTDC), an extra mixing time is available for the pilot injected fuel (from -16 to -3 CAD aTDC) which provides a better fuel/air mixture stratification at the start of spark in comparison with the single injection strategy, whose mixing time available corresponds with the injection duration (4 CAD). Once the spark has ignited the mixture, the flame front propagates through a region with a leaner local equivalence ratio. Figure 4 shows the fuel mass distribution at the time of the spark for a single and double injection strategy. It is possible to identify two zones for the double injection strategy at the time of SOC (dashed blue trace). The first zone containing the mixture below stoichiometric equivalence ratio ($0.2<\phi<0.5$) is attributed to the pilot injection, which has had enough mixing time to reach a leaner mixture distribution. The second zone, with equivalence ratio ($\phi>0.5$) is attributed to the extra fuel mass provided by the main injection. As it is possible to appreciate, the local conditions near stoichiometric needed to ignite the mixture with the spark plug are achieved by the fuel mass injected in the main injection. If there is not a main injection, no ignition is achieved due to the excessively lean mixture created by the pilot injection.

Looking at the NOx-Soot trade-off in Figure 3, it can be seen that higher levels of soot are obtained in the cases using the single injection strategy. The start of combustion, provided by the spark plug discharge, occurs at the end of the injection event providing a short mixing time. The flame front propagates in a region of rich equivalence ratios with a high quantity of the mass mixed above

stoichiometric conditions, promoting increased soot formation. On the other hand, Figure 4 shows how the extra mixing time achieved with the double injection strategy results in a regions in the chamber with local leaner equivalence ratios. This reduces soot formation and lowers the soot values as shown in Figure 3.

Depending on the global equivalence ratio used, the extra mixing time from the pilot to the main injection can promote an over-mixing condition which generates high levels of CO and HC. In this case is it possible to reduce the over-mixing effect by increasing the fuel mass amount in the main injection in order to promote the flame growth. Another possible solution to reduce the over-mixing effect is to increase the global equivalence ratio, limited by the knocking level. When a reactive enough conditions are set, the knocking level is increased as the fuel mass in the pilot injection increases due to the larger and faster heat release rate in the autoignition phase.

The NOx-ISFC trade off is clearly improved with the use of the double injection strategy. As it will be described in the next section, the double injection strategy enhances both phases of the combustion allowing an improvement in the Fuel energy Conversion Efficiency (FeCE). The FeCE, or combustion efficiency, estimates the quantity of fuel burned during the combustion process and it is calculated by means of the engine-out emissions measurements, in particular:

$$\mathbf{FeCE} = \left(\mathbf{1} - \left(\frac{\mathbf{uHC}}{\mathbf{mf}}\right) - \left(\frac{\mathbf{CO}}{\mathbf{4 \cdot mf}}\right)\right) \cdot \mathbf{100} \quad (3)$$

4. EVALUATION OF THE COMBUSTION CONCEPT USING A DOUBLE INJECTION STRATEGY

A general overview of the double injection strategy's potential was presented in the preliminary results. In this section, a deeper analysis of the effects of this injection strategy will be presented. For this purpose, a different set of experimental results are shown and discussed. In a first step, the effects of

275 the dwell between the pilot and main injection in a split injection strategy (50% fuel mass amount in
276 each injection) as well as the effects of the XO_2 variation are analysed. In a second step, the effects of
277 the fuel mass distribution between the pilot and main injection are studied.

278

279 **4.1 Effect of dwell variation and oxygen concentration**

280 The mixing process prior to the start of combustion has a strong effect on the combustion development.
281 In order to quantify these effects in terms of performance and emissions, different tests were
282 performed. As depicted in Table 3, the pilot injection was swept from -31 to -16 CAD aTDC, while
283 maintaining constant injection pressure at 900 bar (to ensure a combustion development during the
284 expansion stroke minimizing NOx emissions), global equivalence ratio (ϕ_g=0.4) and start of the main
285 injection (-9 CAD). Considering the gasoline direct injection literature and author's experience, the spark
286 discharge is set at the end of the main injection in all cases in order operate within the "ignitability
287 window" range. That is, if start of spark is located before the end of injection, excessive rich equivalence
288 ratio are attained in the gap of the spark electrodes. By contrast, if the start of spark is set after the end
289 of injection, excessive lean equivalence ratios are achieved. In both cases the combustion development
290 is worsened leading a misfiring. Finally, a sweep of the intake XO_2 was performed for the three
291 conditions with higher FeCE to determine its effect on the FeCE and ISFC.

292 Figure 5 shows the FeCE, IMPG, IMEP and ISFC versus the pilot injection timing. The black trace depicts
293 the cases with an intake XO_2 of 19.6%. For the cases where the pilot timing is -16, -19 and -22 CAD, a
294 sweep of the intake XO_2 from 19.6% down to 17.2% in steps of 0.4% is presented. The red horizontal
295 dashed trace across the figure denotes the reference results for the single injection strategy with the
296 same engine operating conditions and with the start of injection fixed at -9 CAD aTDC. Taking into
297 account the high NOx levels presented in the preliminary results for the single injection strategy, the
298 injection timing has been located (at -9 CAD aTDC) looking for a combustion development close to the

299 expansion stroke, which imply a combustion development under lower combustion temperatures
300 minimizing the NOx emission levels. Figure 6a shows the crank angle evolution of different variables.
301 From the top to the bottom, the figure shows the mass flow rate, the mean unburned gas temperature,
302 the in-cylinder pressure and the rate of heat released. In all cases, the spark plug discharge was set at
303 EoI and it determines the SoC. Figure 6b displays the mixture distribution for three different pilot
304 injection cases. Additionally, Figure 7 presents the results in terms of soot, CO, HC and NOx as a function
305 of the pilot injection timing.

306 The FeCE trend in Figure 5 reveals that the maximum FeCE value is obtained for the case in which the
307 pilot injection is set at -22 CAD. At this point, the optimum conditions in terms of FeCE are achieved for
308 this injection strategy and the range of injection timings tested. The resulting mixture conditions allows
309 a powerful autoignition after the flame propagation phase which leads to higher in-cylinder pressure
310 and temperature as Figure 6a shows. Taking into account the evolution of the FeCE it is possible to note
311 that, for the global equivalence ratio tested (ϕ_g=0.4), the over-mixing effect is magnified as the pilot
312 injection is advanced from -22 CAD to -31 CAD. It results in a 20% reduction in the FeCE for that case.
313 The over-mixing effect promotes a retarded location of the combustion event in the cycle (Figure 6a)
314 which causes a halving in the IMEP value compared with the single injection case. The combination of
315 the lower combustion efficiency and the retarded combustion timing results in a value of the ISFC which
316 is almost double than the one obtained with the single injection case.

317 Focusing on Figure 5, it is interesting to note that the double injection strategy provides a higher FeCE
318 than the reference case of the single injection strategy for all the points except for the case of SoI_{pilot}= -
319 28 CAD aTDC and SoI_{pilot}= -31 CAD aTDC. In that case (SoI_{pilot}= -31 CAD aTDC) the mixture conditions in
320 the surrounding areas at SoC (Figure 6b) have become too lean, hinder the flame propagation and
321 avoiding the autoignition of the rest of the mixture. Thus, a soft combustion development shifted to the

expansion stroke is attained in this case, which results in a rapid decay in the FeCE due to the incomplete combustion (Figure 5). For all the other cases, the main injection event provides the necessary conditions to start the combustion event after the spark plug has discharged.

As a general trend, the IMEP and ISFC values correlate well with the FeCE values. As Figure 6a shows, the combustion phasing is similar for SoI_{pilot}= -22 CAD aTDC (8.9 CAD) and SoI_{pilot}= -16 CAD aTDC (9.9 CAD), but the slightly higher FeCE value for SoI_{pilot}= -22 CAD aTDC provides a slight value of IMEP. For the advanced Start of pilot Injection cases (-31, -28 and -25 CAD), the retarded phasing of the RoHR causes a strong reduction in the IMEP values and a consequent increase in the specific fuel consumption.

Regarding the knocking level, the IMPG level is negligible for the advanced SoI pilot cases due to the poor combustion attained, which can be appreciated in the high HC and CO emissions showed in Figure 7. As the pilot injection is moved closer to the main injection (retarded), the higher reactivity allows an improvement in the combustion process resulting in a stronger autoignition, which provokes higher knock values. The SoI_{pilot}= -22 CAD aTDC presents the best combustion efficiency and also gives the highest IMPG or knock value due to the high pressure rise rate created by the strong autoignition.

In terms of engine-out emissions (Figure 7), for the early pilot injection cases (-31, -28 and -25 CAD), the poor FeCE values cause high CO and HC levels as well as low soot and NOx emissions. The trend obtained for the more delayed pilot injection cases is consistent with the values obtained for the FeCE and IMEP.

Focusing on the XO_2 effect it is possible to state that as the intake XO_2 is decreased the combustion process is worsened and the FeCE values decrease, as the individual symbols in Figure 5 show. For the SoI_{pilot}= -22 CAD aTDC, the FeCE with the double injection strategy is higher than the one obtained in the single injection strategy for intake XO_2 values above 18.4% (3^{rd} XO_2 reduction step). For the SoI_{pilot}= -19

CAD aTDC and SoI_{pilot}= -16 CAD aTDC the FeCE drops below the single injection strategy level for the first reduction step in the XO_2 (19.2%). It is worthy to note that it is possible to move the engine-out emissions values for the double injection case near the emissions for the single injection case by reducing the intake oxygen concentration.

4.2 Effect of mass distribution

With the aim studying further the effect of the mass distribution between the main and pilot injection on the combustion development and on the performance and pollutant emissions, different tests were performed using the operating conditions shown in Table 4. The single injection strategy reference case depicted in Table 4 was compared with five different mass distributions for the double injection strategy (%pilot/%main: 40%/60%, 45%/55%, 50%/50%, 55%/45% and 60%/40%). As it is possible to appreciate by observing the fuel mass flow traces in Figure 8a, which represents the data for three mass distributions and the single injection strategy in the same manner as in Figure 6, the SoI timing of the pilot injection and the EoI timing of the main injection was held constant for all the cases. In addition, the unburned gas temperature, in-cylinder pressure, and rate of heat released for three of the double injection cases are shown in Figure 8a. It should be noted here that the RoHR in Figure 8a is different than the RoHR in Figure 6a because the operating conditions have changed. For the cases in Figure 8a the engine speed is increased and the XO_2 concentration is lowered. Both of these changes contribute to lengthening the duration of the heat release.

Figure 8b shows a distribution of fuel mass fraction versus ϕ calculated using the 1-D mixing model described above at the experimental SoC time (up) and at the autoignition time (down) for the same engine settings shown in Figure 8a. Figures 9 and 10 show the performance and engine-out emissions obtained from the five cases as well as the results obtained from the single injection reference case (red horizontal dashed trace) using the conditions shown in Table 4.

It is worthy to note that, in this study, the baseline operating conditions for the single injection strategy are notably different from the baseline operating conditions used in subsection 4.1 (Table 3). In this case, the in-cylinder conditions are set in order to deteriorate the combustion process. These conditions allow to magnify both, the double injection potential in comparison with the single injection strategy as well as the influence of the mass distribution on the combustion development. Thus, the global equivalence ratio as well as the intake XO_2 are fixed in a lower value (ϕ_g=0.36 instead of ϕ_g=0.4, and XO_2=18% instead of XO_2=19.6%). In addition engine speed was set at 1500 rpm. These have a strong effect on the combustion development as it can be seen by comparing both RoHR profiles (Figure 6a versus Figure 8a).

As Figure 8a shows, the SoC is slightly advanced as the amount of fuel injected in the main injection is increased ($CA10_{40/60}$= 5 CAD < $CA10_{50/50}$= 6 CAD < $CA10_{60/40}$= 7.2 CAD) due to the higher amount of fuel mass mixed under reactive conditions, as it is stated in the mixture mass fraction histograms in Figure 8b (up and down). The rise in the RoHR during the flame propagation phase (from 0 to +10 CAD aTDC) is quite similar independent on the fuel mass distribution. Moreover, the location of the RoHR peak in the flame propagation phase is achieved between +8 to +10 CAD aTDC for the three cases presented. This maximum level of the RoHR is higher for the case with lower fuel mass amount injected in the pilot injection. It can be noted that for the double injection cases studied, in which a lean global equivalence ratio is used, the flame propagation is enhanced as the amount of fuel/air mixture near reactive equivalences ratios at SoC (Figure 8b up) is increased, preventing the over-mixing.

It is possible to observe that two combustion phases are achieved only in the case in which the lower amount of fuel mass is injected in the pilot event (green traces). The higher in-cylinder pressure and unburned temperature in the combustion chamber at the end of the first combustion phase combined with the higher fuel mass injected in the main injection results in a more energetic autoignition (51

390 J/CAD versus 32 J/CAD and 31 J/CAD). In the 50%/50% case a soft change in the RoHR profile is observed
391 at +15 CAD aTDC, being this change in the RoHR slope negligible in the case of 60%/40%.

392 Regarding the air/fuel mixing process shown in Figure 8b, two zones can be identified at the time of SOC
393 (Figure 8b up). The first zone containing the mixture below stoichiometric equivalence ratio ($\phi<1$) is
394 attributed to the pilot injection, which has had enough mixing time to reach a leaner mixture
395 distribution. The second zone, with equivalence ratio higher than stoichiometric ($\phi>1$) is attributed to
396 the extra fuel mass provided by the main injection. The fuel mass amount mixed in the high reactivity
397 zone ($1<\phi<2$) increases as the percentage of fuel injected in the main injection increases. This enhances
398 the first reactions after the spark discharge leading to development of the premixed flame and
399 consequently causes a faster start of combustion. As the mass distribution at the autoignition time
400 (Figure 8b down) shows, a lower mass percentage in the main injection provides additional leaner
401 mixture, and as a consequence a smoother autoignition phase is obtained. In summary, the case with
402 the lowest percentage in the main (red trace) has a very poor autoignition phase, the case with 50% in
403 the main (blue trace) shows a soft autoignition, and the case with 60% in the main (green trace) shows
404 the strongest autoignition.

405 Figure 9 shows the benefit obtained in the case of the double injection strategy by varying the fuel mass
406 amount injected in each injection event in comparison with the single injection strategy at the same
407 operating condition. The FeCE was similar for the single injection and the double injection cases with all
408 of the values between 84% and 90%. As the RoHR profiles in Figure 8a point out, an improvement in the
409 combustion development is attained by using the double injection strategy in comparison with the
410 single injection strategy. Thus, higher IMEP values were obtained, allowing a reduction in the ISFC by
411 approximately 150 g/kWh.

412 Comparing the performance and engine-out emissions for the double injection strategies in Figures 9
413 and 10, there is an improvement in the efficiency as the pilot injected mass decreases. For the cases
414 studied, in which a lean global equivalence ratio is used (ϕ_g=0.36), the larger amount of fuel injected in
415 the main event enhances the flame propagation once the combustion has started. The benefit obtained
416 in the mixing process is reflected in a better combustion process as the FeCE and IMEP values show and
417 therefore lower ISFC values are obtained. Regarding the knock level, IMPG is lower in the case with the
418 larger amount of fuel injected in the pilot injection. In this case, a soft autoignition shifted to the
419 expansion stroke is obtained as a consequence of the over-mixing effect.

420 Comparing single and double injection strategies in terms of engine-out emissions, it is demonstrated
421 that depending on the mass distribution selected for the double injection, the improvement obtained in
422 comparison with the single injection strategy can be more or less noticeable. More improvement in
423 terms of HC, CO and ISFC in comparison to the single injection strategy is obtained in the case with the
424 lower fuel amount injected in the pilot injection. Higher FeCE implies higher temperatures and therefore
425 higher NOx as well as lower CO and HC levels. This enhancement in the combustion development is
426 allowed by the more reactive ambient provided by the fuel stratification due to the pilot injection
427 (Figure 8b) in which the main injection takes place. By contrast, in the case of the larger fuel amount
428 injected in the pilot injection (60% pilot/40% main) a leaner mixture is obtained and the flame front
429 propagation is slowed down causing high CO and HC values. Regarding soot emissions, quite similar
430 levels for all five fuel distributions studied has been obtained.

431

432 5. CONCLUSIONS

433 The analysis of the parameters derived from the in-cylinder pressure and the engine-out emissions
434 measurements shows the usefulness of the double injection strategy applied to the Spark Assisted

435 Partially Premixed Compression Ignition combustion mode fuelled with high ON gasoline under light
436 load operating conditions. A 1-D jet mixture distribution model calculation was used to explain some
437 trends that were observed.

438 Two studies were performed to assess the potential of the double injection strategy. First, a sweep of
439 the pilot injection timing was done while fixing the main injection timing. As part of this study, a sweep
440 of the intake XO_2 concentration has been done at several points. Taking into account the global lean
441 equivalence ratio used during the tests, two different scenarios has been found:

442 - On the one hand, when advanced pilot injection timings are set, too lean mixture conditions at
443 SoC are obtained. These conditions hind the flame propagation and avoid the autoignition of the
444 rest of the mixture leading a deteriorated combustion development shifted to the expansion
445 stroke. A rapid decay in the FeCE due to the incomplete combustion is obtained increasing the
446 CO and HC emission levels. In this case, double injection do not provide better results than the
447 single injection strategy. Due to the poor combustion development, lower NOx and soot
448 emission levels are obtained.

449 - On the other hand, the use of more delayed pilot injection timings provides the necessary
450 conditions at the start of combustion, preventing the over-mixing. The better air/fuel mixture
451 distribution enhances the combustion development improving the IMEP and and lowering the
452 CO and HC emissions (higher FeCE) in comparison with the single injection strategy. Higher NOx
453 and soot emission levels are obtained too.

454 In a second study, five different mass distributions between the pilot and main injection were evaluated.
455 Having in mind the lean global equivalence ratio used (ϕ_g=0.36), it is possible to state that:

- By increasing the mass percentage in the main injection the over-mixing effect is avoided. The more reactive conditions at SoC improve significantly the combustion process, providing higher IMEP values and consequently reducing the ISFC. Therefore, higher NOx and lower CO and UHC emissions were obtained.

- In terms of IMEP and ISFC, all the five mass distributions tested with the double injection strategy improved the results in comparison with the single injection strategy.

As a general conclusion, it has been demonstrated that the better air/fuel mixture distribution obtained using double injection strategies, in comparison with the single injection strategy, enhances the combustion development improving the Fuel energy Conversion Efficiency. Thus, the use of the double injection strategy allows to widen the PPC with spark assistance operating range in low load conditions. It is worthy to note that in this light load operating conditions no autoignition is achieved without the use of the spark assistance. Finally, it is important to remark that the present work was carried out without any optimization in terms of engine hardware settings and consequently more research is needed to found the optimum conditions.

ACKNOWLEDGMENTS

The authors would like to thank General Motors for supporting this research.

REFERENCES

[1] Kimura S, Aoki S, Kitahara Y, Aiyoshizawa E. Ultra-clean Combustion Technology Combining a Low-temperature and Premixed Combustion Concept for Meeting Future Emission Standards, SAE International, SAE 2001-01-0200, 2001.

[2] Singh AP, Agarwal AK. Combustion characteristics of diesel HCCI engine: an experimental investigation using external mixture formation technique. Appl Energy 2012.

[3] Law D, Kemp D, Allen J, Kirkpatrick G, Copland T. Controlled combustion in an IC-engine with a fully variable valve train. SAE paper 2001-01-0251; 2001.

[4] Agrell F, Ångström H-E, Eriksson B, Wikander J, Linderyd J. Integrated simulation and engine test of closed loop HCCI control by aid of variable valve timings. SAE paper 2003-01-0748; 2003.

[5] Haraldsson G, Tunestål P, Johansson B, Hyvönen J. HCCI combustion phasing in a multi cylinder engine using variable compression ratio. SAE paper 2002-01-2858; 2002.

[6] Maurya R K, Agarwal A K. Experimental investigation on the effect of intake air temperature and air–fuel ratio on cycle-to-cycle variations of HCCI combustion and performance parameters. Applied Energy, Vol. 88, pp 1153-1163, 2011.

[7] Yang J, Culp T, Kenney T. Development of a Gasoline Engine System Using HCCI Technology e the Concept and the Test Results, SAE paper 2002-1-2832.

[8] Kalghatgi G, Kumara Gurubaran R, Davenport A, Harrison AJ, Hardalupas Y, Taylor AMKP. Some advantages and challenges of running a Euro IV, V6 diesel engine on a gasoline fuel. Fuel, Vol. 108, pp 197-207, 2013.

[9] Yu C, Wang J, Wang Z, Shuai S. Comparative study on Gasoline Homogeneous Charge Induced Ignition (HCII) by diesel and Gasoline/Diesel Blend Fuels (GDBF) combustion. Fuel, Vol. 106, pp 470-447, 2013.

[10] Risberg P, Kalghatgi G, Ångstrom H, Wåhlin F. Auto-ignition quality of Diesel-like fuels in HCCI engines. SAE Technical Paper 2005-01-2127, 2005.

[11]Kalghatgi G, Risberg P, Ångström H. Advantages of Fuels with High Resistance to Auto-ignition in Lateinjection, Low-temperature, Compression Ignition Combustion. SAE Technical Paper 2006-01-3385, 2006.

[12]Kalghatgi G, Risberg P, Ångström H. Partially Pre-Mixed Auto-Ignition of Gasoline to Attain Low Smoke and Low NOx at High Load in a Compression Ignition Engine and Comparison with a Diesel Fuel. SAE Technical Paper 2007-01-0006, 2007.

[13]Kalghatgi G. Low NOx and Low Smoke Operation of a Diesel Engine using Gasoline-Like Fuels. ASME International Combustion Engine Division 2009 Spring Technical Conference, ICES2009-76034, 2009.

[14]Manente V, Johansson B, Tunestal P. Partially Premixed Combustion at High Load using Gasoline and Ethanol, a Comparison with Diesel. SAE Technical Paper 2009-01-0944, 2009.

[15]Manente V, Johansson B, Tunestal P. Half Load Partially Premixed Combustion, PPC, with High Octane Number Fuels. Gasoline and Ethanol Compared with Diesel. SIAT 2009 295, 2009.

[16]Manente V, Johansson B, Tunestal P. Characterization of Partially Premixed Combustion with Ethanol: EGR Sweeps, Low and Maximum Loads. ASME International Combustion Engine Division 2009 Technical Conference, ICES2009-76165, 2009.

[17]Manente V, Tunestal P, Johansson B, Cannella W. Effects of Ethanol and Different Type of Gasoline Fuels on Partially Premixed Combustion from Low to High Load. SAE Technical Paper 2010-01-0871, 2010.

[18]Ra Y, Yun J E, Reitz R. Numerical Simulation of Diesel and Gasoline-fueled Compression Ignition Combustion with High-Pressure Late Direct Injection. Int. J. Vehicle Design, Vol. 50, Nos. 1,2,3,4. pp.3-34, 2009.

[19]Ra Y, Yun J E, Reitz R. Numerical Parametric Study of Diesel Engine Operation with Gasoline. Comb. Sci. and Tech., 181:350-378, 2009.

525 [20]Dempsey A, Reitz R. Computational Optimization of a Heavy-Duty Compression Ignition Engine
526 Fueled with Conventional Gasoline. SAE Int. J. Engines 4(1):338-359, 2011, doi:10.4271/2011-01-
527 0356.
528 [21]Ra Y, Loeper P, Reitz R, Andrie M, et al. Study of High Speed Gasoline Direct Injection Compression
529 Ignition (GDICI) Engine Operation in the LTC Regime. SAE Int. J. Engines (1):1412-1430, 2011.
530 [22]Ra Y, Loeper P, Andrie M, Krieger R, et al. Gasoline DICI Engine Operation in the LTC Regime Using
531 Triple- Pulse Injection. SAE Int. J. Engines 5(3):1109-1132, 2012.
532 [23]Ciatti S, Subramanian S. An Experimental Investigation of Low Octane Gasoline in Diesel Engines.
533 ASME International Combustion Engine Division 2010 Technical Conference, ICEF2010-35056, 2010.
534 [24]Das Adhikary B, Ra Y, Reitz R, Ciatti S. Numerical Optimization of a Light-Duty Compression Ignition
535 Engine Fuelled With Low-Octane Gasoline. SAE Technical Paper 2012-01-1336, 2012.
536 [25]Ciatti S, Johnson M, Das Adhikary B, Reitz R, et al. Efficiency and Emissions performance of
537 Multizone Stratified Compression Ignition Using Different Octane Fuels. SAE Technical Paper 2013-
538 01-0263, 2013.
539 [26]Benajes J, García A, Domenech V, Durrett R. An investigation of partially premixed compression
540 ignition combustion using gasoline and spark assistance. Applied Thermal Engineering Vol 52 p. 468–
541 477; 2013.
542 [27]Pastor JV, García-Oliver JM, García A, Micó C, Durrett R. A spectroscopy study of gasoline partially
543 365 premixed compression ignition spark assisted combustion. Applied Energy, Vol. 104, pp 568-
544 575, 366 2013.
545 [28]Desantes JM, Payri R, García A, Monsalve-Serrano J. Evaluation of Emissions and Performances from
546 Partially Premixed Compression Ignition Combustion using Gasoline and Spark Assistance. SAE paper
547 2013-01-1664; 2013.

[29]Weall A, Collings, N. Gasoline Fuelled Partially Premixed Compression Ignition in a Light Duty Multi Cylinder Engine: A Study of Low Load and Low Speed Operation. SAE Int. J. Engines 2(1):1574-1586, 2009.

[30]Das Adhikary B, Reitz R, Ciatti S. Study of In-Cylinder Combustion and Multi-Cylinder Light Duty Compression Ignition Engine Performance Using Different RON Fuels at Light Load Conditions. SAE Technical Paper 2013-01-0900, 2013.

[31]Desantes JM, Pastor JV, García-Oliver JM, Pastor JM. A 1D model for the description of mixing-controlled reacting diesel sprays. Combustion and Flame 2009; 156:234–49.

[32]Lapuerta M, Armas O, Hernández JJ. Diagnostic of D.I. Diesel Combustion from In-Cylinder Pressure Signal by Estimation of Mean Thermodynamic Properties of the Gas. Applied Thermal Engineering. Vol 19 Nº 5 p. 513–529; 1999.

[33]Payri F, Molina S, Martín J, Armas O. Influence of measurement errors and estimated parameters on combustion diagnosis. Applied Thermal Engineering Vol 26 Nº 2-3 p. 226–236; 2006.

[34]Brecq G, Le Corre O. Modeling of In-cylinder Pressure Oscillations under Knocking Conditions: Introduction to Pressure Envelope Curve. SAE paper 2005-01-1126; 2005.

[35]Borg JM, Alkidas AC. Characterization of Autoignition in a Knocking SI Engine Using Heat Release Analysis. SAE paper 2006-01-3341; 2006.

[36]Eng JA. Characterization of Pressure Waves in HCCI Combustion. SAE paper 2002-01-2859; 2002.

[37]Sjöberg M, Dec JE. Effects of Engine Speed, Fueling Rate, and Combustion Phasing on the Thermal Stratification Required to Limit HCCI Knocking Intensity. SAE paper 2005-01-2125; 2005.

[38]Pastor JV, López JJ, García JM, Pastor JM. A 1D model for the description of mixing-controlled inert diesel sprays. SAE paper 2005-01-1126; 2005.

ABBREVIATIONS

573 bTDC: before Top Dead Center

574 CAD: Crank Angle Degree

575 CA10: Cranck Angle at 10% mass fraction burned

576 CI: Compression Ignition

577 DI: Direct Injection

578 EI: Emission Index

579 EOI_{main}: End of main injection

580 EOI_{pilot}: End of pilot injection

581 FeCE: Fuel energy Conversion Efficiency

582 FFT: Fast Fourier Transform

583 FSN: Filter Smoke Number

584 HCCI: Homogeneous Charge Compression Ignition

585 IMPG: Integrate Modulus of Pressure Gradient

586 ISFC: Indicates Specific Fuel Consumption

587 LTC: Low Temperature Combustion

588 PCCI: Premixed Charge Compression Ignition

589 PPC: Partially Premixed Charge

590 SoC: Start of Combustion

591 SOI_{main}: Start of main injection

592 SOI_{pilot}: Start of pilot injection

593 SoS: Start of Spark

594 TDC: Top Dead Center

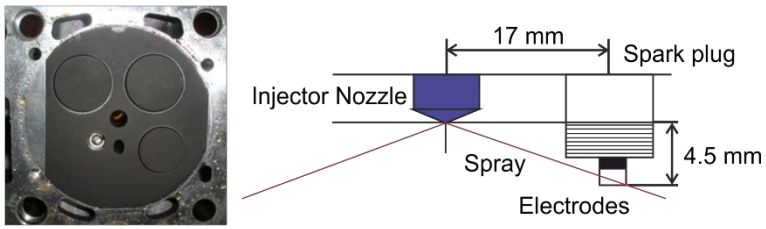

Figure 1. Image of the modified cylinder head with spark plug and injector hole (left). Diagram of the relative position between the injector and spark plug (right)

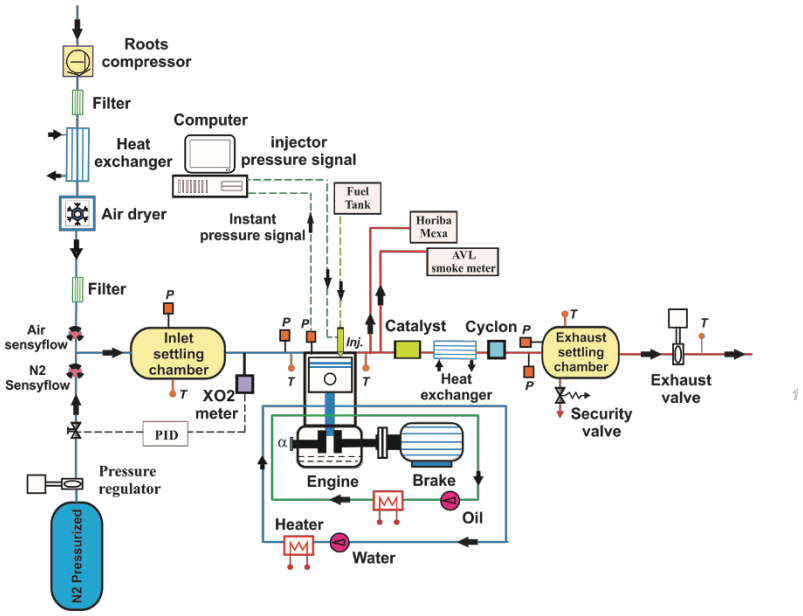

Figure 2. Complete test cell setup

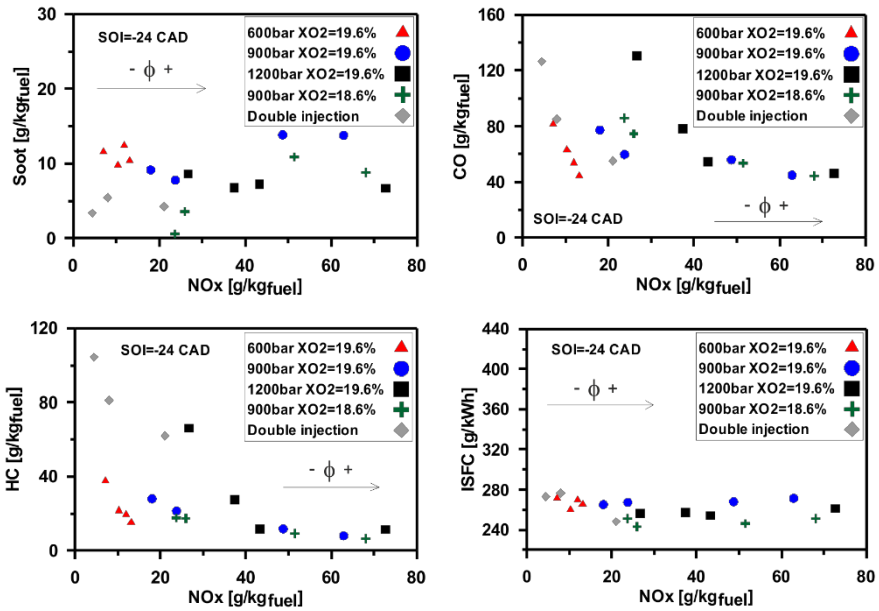

Figure 3. NOx vs HC, SOOT, CO and ISFC trade-off for the injection timing SoI=-24 CAD

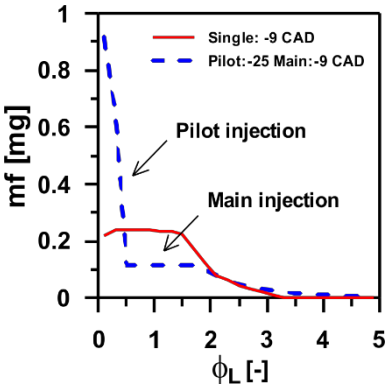

Figure 4. Fuel mass Distribution vs. ϕ at the spark discharge time. Pilot injection: -25 CAD, Main injection: -9 CAD

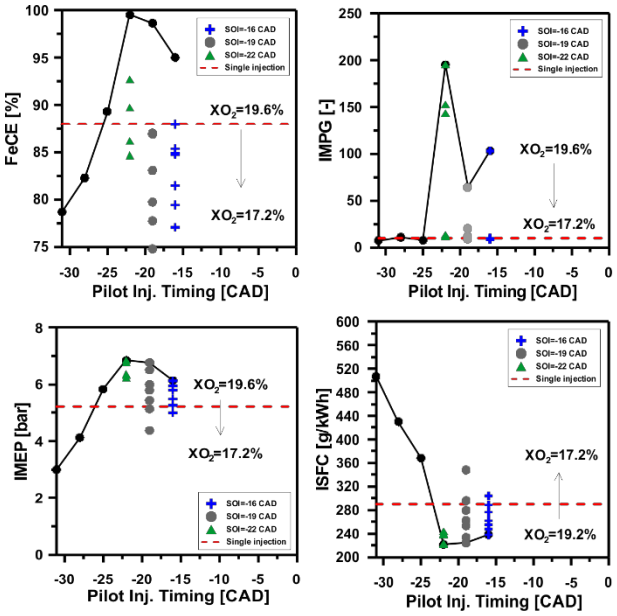

Figure 5. FeCE, IMPG, IMEP and ISFC results for the double injection strategy and the single injection strategy reference case (dashed line). Main injection timing fixed at -9 CAD and pilot injection timing swept from -31 to -16 CAD in steps of 3 CAD

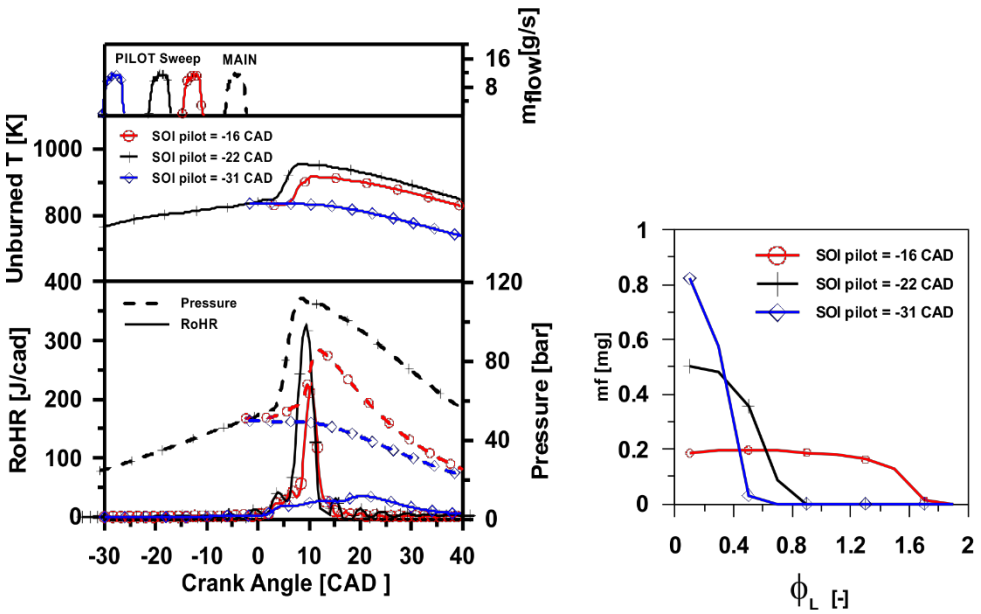

Figure 6. Crank angle evolution of the mass flow rate, unburned gas temperature, in-cylinder pressure, and rate of heat released for the double injection strategy. Main injection timing fixed at -9 CAD and pilot injection timing as shown in legend. Intake XO_2 = 19.6% for all cases

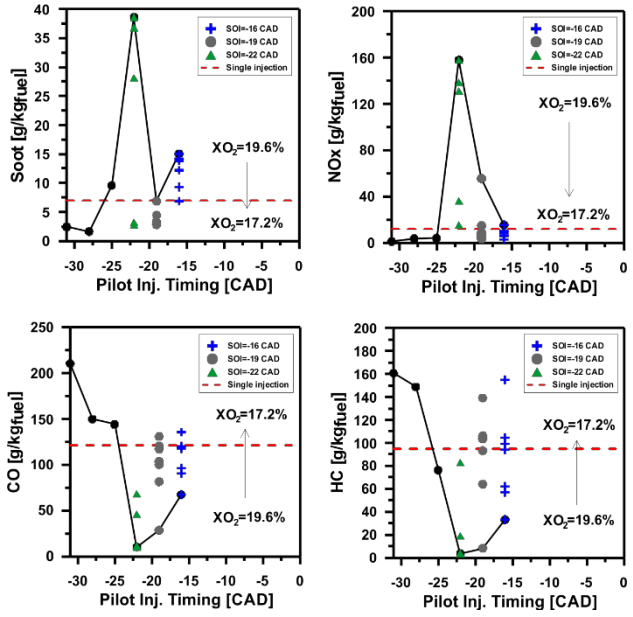

Figure 7. Soot, NOx, CO and HC results for the double injection strategy and the single injection strategy reference case (dashed line). Main injection timing fixed at -9 CAD and pilot injection timing swept from -31 to -16 CAD in steps of 3 CAD

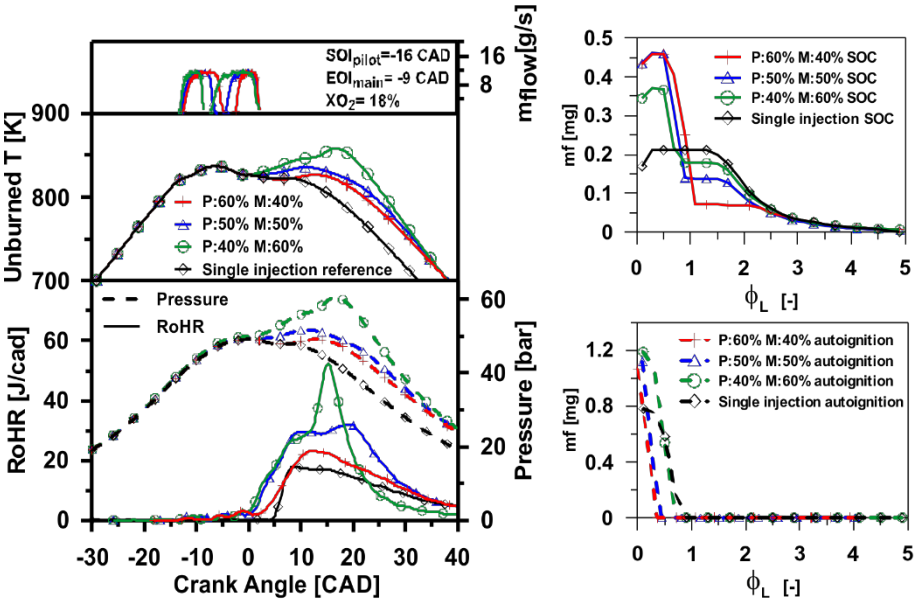

Figure 8. Crank angle evolution of fuel mass flow rate, unburned gas temperature, in-cylinder pressure, and rate of heat released for 40/60, 50/50 and 60/40 fuel mass distribution (7a). Distribution of fuel mass vs. ϕ in experimental SoC (up) and autoignition time (down) for the same fuel mass distributions (7b)

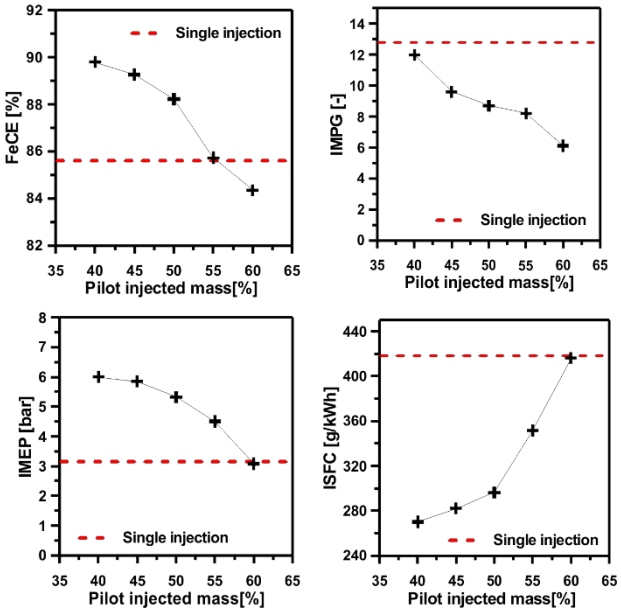

Figure 9. FeCE, IMPG, IMEP and ISFC results for the double injection strategy and the single injection strategy reference case (dashed line). 40/60, 45/55, 50/50, 55/45, 60/40 fuel mass distribution between the main and pilot injection

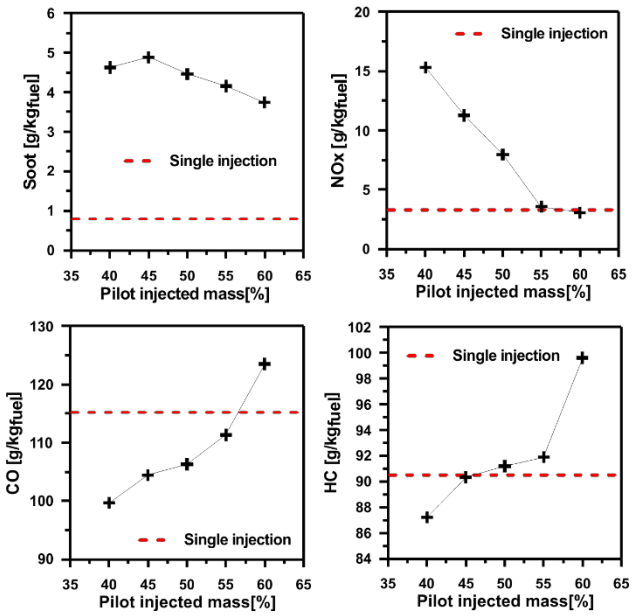

Figure 10. Soot, NOx, CO and HC results for the double injection strategy. 40/60, 45/55, 50/50, 55/45, 60/40 fuel mass distribution between the main and pilot injection

Engine		Injection system		Fuel	
Type	CI, 4stroke, DI	**Type**	CR	**Type**	Gasoline
Cylinder number	1	**Injector**	Bosch CRIP 3.3		
Bore x Stroke	85 x 96 mm	**Hole number**	7	**Density**	722 kg/m^3
Compression ratio	14.7:1	**Included angle**	154^o	**Viscosity**	0.37 mm^2/s
Bowl diameter x depth	45 x 18 mm	**Hole diameter**	97 um	**RON**	98 [-]
Displacement	545 cm^3	**Flow capacity**	210 cm^3/30 s	**Lower HV**	44542 kJ/kg

Table 1. Main characteristics: single cylinder engine, injection system and fuel

	Study	**Pinj [bar]**	**Engine Speed [rpm]**	**Inj.Timing [^{o} aTDC]**	**Spark Timing**	**Intake XO_2 [%]**	**Global ϕ [-]**
Single injection	P_{inj} variation	600	1500	-24	EOI	19.6	0.3-0.55
		900					0.3-0.55
		1200					0.25-0.75
	XO_2 variation	900				18.6	0.3-0.36
						19.6	0.22-0.3
Double injection	P:35% M:65%	900	1500	SOI pilot: -16 EOI main: -3	EOI main	18	0.36
	P:65% M:35%						
	P:50% M:50%						

Table 2. Operating conditions for the single injection and double injection strategy preliminary results

	P_{inj} [bar]	**Engine Speed [rpm]**	**Pilot Inj. [^{o} aTDC]**	**Main Inj. [^{o} aTDC]**	**Spark Timing**	**Intake XO_2 [%]**	**Global ϕ [-]**
Double injection	900	1000	-16	-9	EOI main	19.6	0.4
			-19			19.6 to	
			-22			19.6 to	
			-25			19.6	
			-28			19.6	
			-31			19.6	
Single injection	900	1000	-	-9	EOI main	19.6	0.4

Table 3. Operating conditions tested to evaluate the effect of dwell and oxygen concentration

		P_{inj} [bar]	Engine Speed [rpm]	Inj.Timing [^{o} aTDC]	Spark Timing	Intake XO_2 [%]	Global ϕ [-]
Double	P:40% M:60%	900	1500	SOI pilot: -16 EOI main: -3	EOI main	18	0.36
	P:45% M:55%						
	P:50% M:50%						
	P:55% M:45%						
	P:60% M:40%						
Single				-9	EOI		

Table 4. Operating conditions for the mass distribution sweep using the double injection strategy